

Transient EPR and Absorption Studies of Carotenoid Triplet Formation in Purple Bacterial Antenna Complexes

Robert Bittl,^{*,†} Eberhard Schlodder,[†] Irene Geisenheimer,[†] Wolfgang Lubitz,[†] and Richard J. Cogdell[‡]

Max-Volmer-Laboratorium für Biophysikalische Chemie, Technische Universität Berlin, Strasse des 17. Juni 135, 10623 Berlin, Germany, and Division of Biochemistry and Molecular Biology, Davidson Building, University of Glasgow, Glasgow G12 8QQ, U.K.

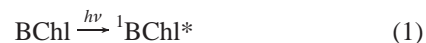
Received: September 16, 2000; In Final Form: March 14, 2001

The dynamics of triplet excited states in light harvesting complexes from a range of different purple bacteria have been investigated by time-resolved EPR and optical absorption spectroscopy. The spin-polarized EPR spectra show for the LH2 complexes from *Rhodobacter sphaeroides* strains 2.4.1 and G1C at early times after light excitation a superposition of bacteriochlorophyll and carotenoid triplet states. In LH1 complexes from *Rhodospirillum rubrum* and LH2 complexes from *Chromatium purpuratum* and *Rhodopseudomonas acidophila*, only a carotenoid triplet spectrum is observed. In all complexes from every species, a time-dependent change in the polarization pattern of the carotenoid triplet is seen. In those complexes that show a superposition of bacteriochlorophyll and carotenoid triplets, the decay of the bacteriochlorophyll triplet is accompanied by an apparently simultaneous rise of the carotenoid triplet. Transient optical absorption spectroscopy demonstrates identical kinetics for the decay and rise of bacteriochlorophyll and carotenoid triplet states, respectively. The lifetime of the carotenoid triplet state shows only a minor temperature dependence in all species. The rate constant for the rise of the carotenoid triplet state is strongly temperature and species dependent. The triplet energy transfer in LH2 complexes from *Rb. sphaeroides* 2.4.1 is about 1 order of magnitude slower than in *Rps. acidophila*. Even the complexes from the *Rb. sphaeroides* strains 2.4.1 and G1C show differences. In *Rb. sphaeroides* G1C, a partial freezing out of the triplet energy transfer is observed which does not occur in any other investigated complex. The observed temperature dependence of the triplet energy transfer from bacteriochlorophylls to carotenoids is discussed in terms of the distance difference between the carotenoid and the two inequivalent bacteriochlorophyll molecules.

1. Introduction

Carotenoids perform two major functions in photosynthesis.^{1,2} They serve as efficient accessory light-harvesting pigments, absorbing light in the blue-green region of the spectrum and transferring excitation energy to the chlorophylls (Chl) or bacteriochlorophylls (BChl). In this way they broaden the spectral range over which light can drive photosynthesis.^{1,2} Second, they serve as “photoprotectors”, by virtue of their ability to rapidly quench Chl and BChl triplet states, thereby preventing the formation of singlet oxygen and subsequent harmful oxidation events. This second function is the essential role of carotenoids; indeed, without them there would be no photosynthesis in an oxygen-containing environment.

The major photoprotective effect of carotenoids is achieved because they are able to quench the lifetime of the BChl triplet state, ³BChl, for example by about 2 orders of magnitude.^{3–5} This process occurs by way of a triplet energy transfer that can be summarized as follows:



The carotenoid triplet (³Car) state lasts for a few microseconds. Because for all wild-type photosynthetic organisms the energy level of the carotenoid triplet state is below that of singlet oxygen, the carotenoid triplet state cannot sensitize the production of singlet oxygen as far as the triplet energy of the carotenoids is smaller than the transition energy from the triplet ground state of oxygen to its lowest excited singlet state (³Σ_g[−] → ¹Δ_g). It just decays back to the ground state, harmlessly releasing the excess energy as heat. The faster decay observed in the presence of oxygen has been explained by an enhanced intersystem crossing process of the carotenoid triplets induced by oxygen. Carotenoids can also quench singlet oxygen directly,⁶ but the major protective effect in vivo is to prevent singlet oxygen formation.⁷ It is generally accepted that the quenching of BChl triplet states by carotenoids occurs via an electron exchange mechanism.^{7,8} For this to operate, the carotenoids in

* Corresponding author. Fax: +49-30-314-21122. E-mail Robert.Bittl@tu-berlin.de.

[†] Technische Universität Berlin.

[‡] University of Glasgow.

the bacterial photosynthetic pigment–protein complexes, the reaction centers, and the antenna complexes must be located in van der Waals contact with the BChl molecules. The high-resolution structures of the reaction centers and the LH2 complexes determined by X-ray crystallography show that this is indeed the case (for example, see refs 9–11).

Carotenoid triplet formation has been studied in both purple bacterial reaction centers and antenna complexes using a variety of techniques, such as flash photolysis,^{3–5} EPR,^{12,13} and ODMR.¹⁴ However, in most cases either the time-resolution or the signal-to-noise ratio has not been sufficient to allow a detailed study of the events that occur during the time when the carotenoid triplets are formed, i.e., in the first few ns. In a recent report, where this was attempted with time-resolved EPR, looking at the formation of the carotenoid triplet state in either the LH2 complex from *Rhodospseudomonas acidophila* strain 10050 or an artificial carotenoid–porphyrin, unusual spin polarization effects were seen during the lifetime of the carotenoid triplet state.¹⁵ Carbonera et al.¹⁵ showed that the spin polarization pattern of the carotenoid triplet state reversed during its lifetime. Similar events have been described in the reaction centers from *Rhodobacter sphaeroides*.¹⁶

We therefore undertook a detailed study of carotenoid triplet formation in a range of antenna complexes from several different species of purple bacteria using a combination of time-resolved EPR and transient optical absorption spectroscopy to more fully characterize this phenomenon and the detailed events occurring during the triplet energy transfer.

2. Experimental Methods

LH2 complexes were isolated and purified from the following species of purple bacteria, *Rhodospseudomonas acidophila* strain 10050, *Chromatium purpuratum*, and *Rhodobacter sphaeroides* strains 2.4.1 and G1C, as previously described.¹⁷ LH1 was isolated and purified from *Rhodospirillum rubrum* strain S1.¹⁷ In each case, the antenna complex was finally resuspended in 0.1% LDAO (v/v), 20 mM Tris HCl pH 8.0. For the low-temperature studies, glycerol was added to give final concentrations of 60% (v/v) and the sample was rapidly frozen in liquid nitrogen. The intactness of the antenna complexes was checked routinely by monitoring their absorption spectra.¹⁷

The time-resolved EPR spectra were recorded with a Bruker ESP380E X-band EPR spectrometer with an ER4118X-MD5-EN–W1 resonator. The resonator was placed in an Oxford CF935 helium cryostat. A laboratory written acquisition module was used for direct detection EPR without field modulation. Quartz sample tubes of 3 mm inner diameter and 4 mm outer diameter were filled to a sample height of about 1 cm. The excitation source was a Q-switched and frequency doubled ($\lambda = 532$ nm) Spectra Physics GCR 130 Nd:YAG laser. This provided 8 ns (full width at half-maximum) pulses with an incident light energy at the sample of about 10 mJ per pulse at 10 Hz repetition rate. Complete kinetic and spectral data sets were recorded using a Lecroy 9540A digital storage oscilloscope triggered by a photodiode. The data sets typically consisted of 20 μ s (800 data points) transients recorded at 256 magnetic field positions covering a spectral range of 90 mT. The transients had a pretrigger baseline of about 4 μ s. This baseline was set to zero for each individual transient as a first step in the data analysis. The transient spectra were extracted by a numerical box car method, i.e., the signal intensity was averaged for a given time window for each field point. All of the spectra and transients presented in the figures below are plotted such that

absorptive (a) signals are positive and emissive (e) signals are negative with respect to the baseline.

Laser flash induced absorbance changes in the BChl *a* Q_y -region were measured using cw laser diodes (Rohm RLD-85PC at 850 nm and Hitachi HL8318G at 830 nm) as measuring light sources. The laser beam was focused through the cuvette onto the active area of a silicon photodiode (EG&G FND-100). To minimize the amount of flash-induced fluorescence light on the detector, the photodiode was protected by interference and cutoff filters and placed about 1 m behind the sample. After amplification (IV86 amplifier from the Hahn-Meitner-Institut, Berlin; electrical bandwidth: 500 Hz–1 GHz), the signals were digitized and averaged by a transient recorder (Tektronix TDS 540). The minimal fwhm of the instrumental response function was about 4 ns. For measurements with a total sweep of ≥ 10 μ s, an amplifier with a reduced electrical bandwidth of 1 MHz (Tektronix TEK AM502) was used.

Formation and decay of the carotenoid triplet was monitored at 515 nm (*Rb. sphaeroides* strain G1C), 550 nm (*Rps. acidophila* and *Rb. sphaeroides* strain 2.4.1) and 620 nm (*Chr. purpuratum*) using a 75 W cw Xe short arc lamp in combination with the Amko LTI A1075 lamp housing as a measuring light source. The measuring light was focused through an interference filter and the sample onto the photodiode (EG&G FND-100). The detector was protected against scattered actinic flash light by narrow band interference filters and colored glasses. The detection system was the same as described above. Contributions to the signals from fluorescence and/or scattered flash light were measured after switching off the measuring light and were subtracted if necessary.

The samples were excited at 532 nm by 3 ns laser flashes from a frequency-doubled Nd:YAG laser (Quantel YG 441) with pulse energies up to 20 mJ at a repetition rate between 1 and 5 Hz. Low-temperature measurements were made using a liquid nitrogen cryostat (Oxford DN 1704, between 77 and 290 K) or a liquid helium flow cryostat (between 5 and 290 K, Oxford CF1204). The time courses of the absorbance changes were fitted with a sum of exponentials using an algorithm that minimizes the sum of the unweighted least squares.

3. Results

3.1. Time-Resolved EPR. The laser flash induced EPR signals of the antenna carotenoid triplet states were recorded at a variety of temperatures between 20 and 200 K. In each case, spectra were calculated from the data sets at various time intervals following the excitation flashes. A typical set of spectra recorded at 50 K is shown in Figure 1 and serves to illustrate the general pattern of the results. The triplet state zero-field splitting values $|D|$ and $|E|$ calculated from these spectra for the different carotenoid triplet states are given in Table 1 and agree well with literature data.^{14,18}

The most straightforward case to describe first is the LH2 (B830) complex from *Chr. purpuratum* (Figure 1A). In this case the carotenoid present is okenone.¹⁹ The initial spectrum calculated in the time interval from 125 to 500 ns after the laser flash shows an (e/e/a/e/a/a) polarization pattern. By the time of the second spectrum (time interval 2–3.5 μ s after the flash), the signals at the inner two canonical orientations (*x*, *y*) have inverted. The final spectrum in this series (11–15.5 μ s) shows now the polarization pattern (e/a/e/a/e/a). This is the spin polarization pattern previously described by Frank et al.¹² for the carotenoid triplet state in LH2 complexes from *Rb. sphaeroides* under excitation with continuous light.

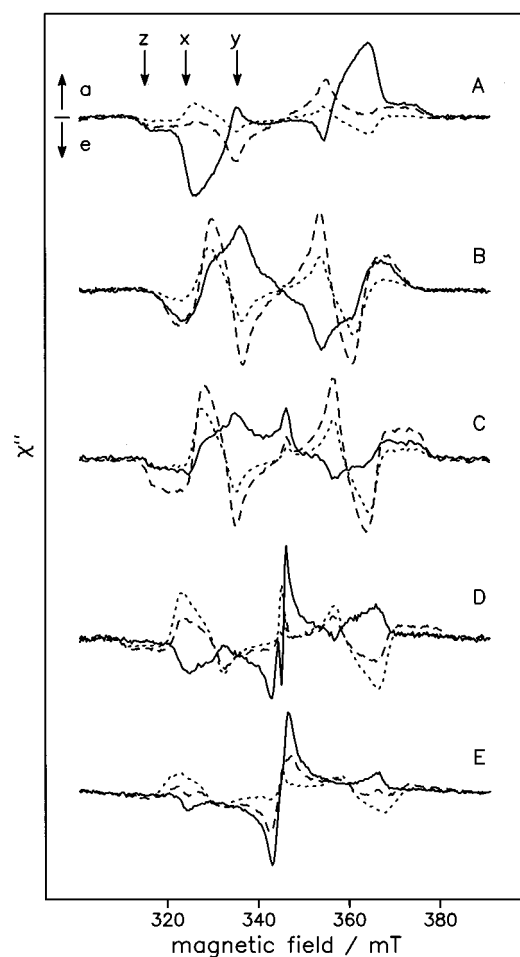


Figure 1. Transient EPR spectra of LH complexes after light excitation in four different preparations. For each preparation three spectra at different times after the light pulse are shown (solid line: 120–500 ns; broken line: 2.0–3.5 μ s; dotted line: 11.0–15.5 μ s. Positive signals indicate microwave absorption (a) and negative signals indicate emission (e). In *Chr. purpuratum* (A), *R. rubrum* (B), and *Rps. acidophila* (C), the spectra show a polarization inversion as a function of time at the inner canonical peaks (y and x) of the Car triplet spectra. In *Rb. sphaeroides* strains 2.4.1 (D) and G1C (E) a transition from BChl *a* triplet spectra to Car triplet spectra is visible. Experimental conditions: $T = 50$ K; microwave frequency $\nu = 9.71$ GHz; 30 dB microwave power attenuation; 256 magnetic field points; 1024, 384, 256, 1024, and 704 transients averaged at each field point for *Chr. purpuratum*, *R. rubrum*, *Rps. acidophila*, *Rb. sphaeroides* strains 2.4.1, and G1C, respectively.

TABLE 1: Triplet Zero-Field Splitting Parameters $|D|$ and $|E|$ (in mT) Calculated from the Transient EPR Spectra for the Carotenoid Triplet States in the LH Complexes Studied (estimated errors ± 0.5 mT)^a

sample	$ D $	$ E $	carotenoid	n
<i>Rb. sphaeroides</i> G1C	39.3	3.8	neurosporene	9
<i>Rb. sphaeroides</i> 2.4.1	35.7	3.7	spheroidene	10
<i>Chr. purpuratum</i>	30.7	3.9	okenone	10
<i>Rps. acidophila</i> 10050	30.3	3.1	rodophin-glucoside	11
<i>R. rubrum</i>	26.0	2.9	spirilloxanthin	13

^a The respective carotenoid in the LH complexes with the corresponding number of conjugated double bonds *n* in the polyene chain are indicated.

A very similar time-dependent change in the polarization pattern of the carotenoid triplet state transient EPR spectrum is seen with the LH1 complex of *R. rubrum* (Figure 1B). In this case the carotenoid is spirilloxanthin,¹⁹ which has 13 conjugated double bonds. The change of the polarization pattern is most

clearly seen, in this case, at the inner canonical resonance. As before, the final polarization pattern is (e/a/e/a/e/a).

The spectra of the carotenoid triplet state in LH2 complexes from *Rps. acidophila* and their time evolution (Figure 1C) closely resemble those of seen for the LH1 of *R. rubrum* (Figure 1B). The main difference is the increased spectral width due to the larger zero-field splittings *D* and *E* for the shorter carotenoid rodophin-glucoside with 11 conjugated double bonds in the LH2 of *Rps. acidophila*. The LH2 sample from *Rps. acidophila* contained a small residual fraction of reaction centers, which gave rise to a narrow disproportionately large $g \approx 2.00$ signal of the light-induced radical pair state $P_{865}^{+}(\text{FeQ}_A^{-})$ ^{20–22} in the center of the spectra. The final polarization pattern of the carotenoid triplet spectrum is as in the case of *Chr. purpuratum* and *R. rubrum* (e/a/e/a/e/a). This is in accordance with the observation in different LH complexes and synthetic carotenoid-porphyrin molecules by cw-EPR.¹⁸

The signals seen with the LH2 complexes from *Rb. sphaeroides* strains 2.4.1 and G1C are more complicated (Figure 1D,E). The rate of carotenoid triplet formation in these two cases is rather slow (see the flash photolysis data below). The LH2 complex from strain 2.4.1 contains the carotenoid spheroidene, which has 10 conjugated double bonds, and the LH2 from strain G1C contains neurosporene, which has 9 conjugated double bonds.¹⁹ Both these LH2 samples also contain a small proportion of reaction centers that give rise to a narrow signal of the light-induced radical pair state $P_{865}^{+}(\text{FeQ}_A^{-})$ most clearly seen in the case of *Rb. sphaeroides* 2.4.1 (Figure 1D). Notwithstanding these complexities, the same time-dependent changes in the polarization pattern of the carotenoid triplet EPR spectra from a (e/e/a/e/a/a) to a (e/a/e/a/e/a) polarization are also seen with these two LH2 complexes. This is best seen in traces D and E in Figure 1 in the field ranges around 324 and 366 mT.

The time dependent changes in the spin polarization patterns of the antenna carotenoid triplet EPR spectra are perhaps most clearly seen looking at the evolution of the transient signals recorded at different field positions. Figure 2 shows three such traces recorded at the three field positions marked by the arrows labeled z, y, x in Figure 1A for the LH2 sample from *Chr. purpuratum*. On the low field, outer canonical resonance z (Figure 2A) the carotenoid triplet formation is fast and complete within the time resolution of the equipment, i.e., ≤ 50 ns. This signal then just decays to the baseline with $t_{1/2} \approx 5.2$ μ s. At this field position the signal remains emissive throughout its lifetime and no change in spin polarization occurs. The time courses at the other two low field, canonical resonances y and x (Figure 2B,C, respectively) also show an initial fast phase; however, in these cases an intermediate phase with $t_{1/2} \approx 1.2$ μ s is seen prior to the decay of the carotenoid triplet state population to the ground state. During this intermediate phase, the direction of the signal inverts showing a change in the spin polarization. The apparent time constants for the polarization change are slightly different at the two field positions.

Figure 3 compares the kinetics of these changes in spin polarization in the LH2 complexes from *Chr. purpuratum* (Figure 3A) and *Rb. sphaeroides* 2.4.1 (Figure 3B) at the inner (y) low field canonical resonance. The LH2 sample from *Rb. sphaeroides* shows an additional initial phase following the laser excitation. Whereas the initial signal intensity in the LH2 sample from *Chr. purpuratum* is absorptive, the initial signal in the LH2 sample of *Rb. sphaeroides* 2.4.1 is emissive. This signal converts with an apparent time constant below 1 μ s into the absorptive signal seen for the *Chr. purpuratum* LH2 sample, to

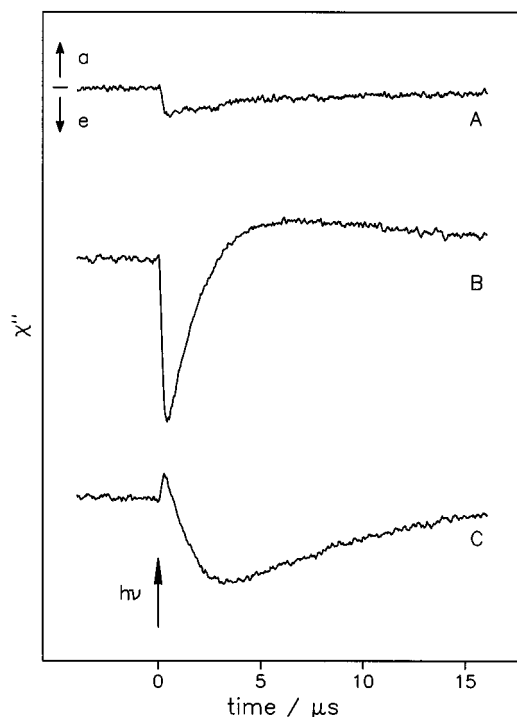


Figure 2. Time evolution of the EPR signal of the Car triplet state in LH2 from *Chr. purpuratum* after light excitation at three different magnetic fields. A: 315.8 mT; B: 325.4 mT; C: 335.2 mT (*z*, *y*, and *x* in Figure 1). Trace A shows a monotonic decay of the EPR signal. Traces B and C show a polarization change at early times after the light flash. Experimental conditions: $T = 50$ K; microwave frequency $\nu = 9.71$ GHz; 30 dB microwave power attenuation; 1024 transients averaged at each field position.

be followed by the same polarization inversion (the signal is now again emissive), and then by the decay of the total triplet state signal.

The inversion of the polarization at the *x* and *y* canonical resonances within the first few μ s after the laser flash occurring in all investigated samples of light harvesting complexes has also been observed in an earlier study on LH2 from *Rps. acidophila* and artificial carotenoid–porphyrin systems.¹⁵ In this study the polarization inversion has been assigned to different depopulation rates of the triplet sublevels. Different depopulation rates of the triplet sublevels have been previously reported for the carotenoid triplet states in reaction centers.¹⁶

An assignment of the additional initial signal contribution in the LH2 sample of *Rb. sphaeroides* 2.4.1 (Figure 3B) is possible by inspection of a very early transient spectrum. Figure 4A shows a transient spectrum calculated in the time interval 100–250 ns after the laser flash. This spectrum has an (e/e/a/a/a) polarization pattern and a width of only about 50 mT compared to the about 70 mT width of the carotenoid spectrum visible in the time interval 2–3.5 μ s (Figure 4B). Due to the limited signal-to-noise ratio of this spectrum, the obtained zero field splitting parameters $D = 47$ mT and $E = 60$ mT have a rather large error margin of about ± 1 mT. In the center of both spectra, narrow features (marked by *) are visible. These are due to the light-induced radical pair state $P_{865}^{+}(FeQ_A^{-})$ in the reaction center part of the sample.^{20–22} In the early spectrum (Figure 4A), this spin polarized $g \approx 2.00$ signal shows an (e/a) polarization pattern that converts to a purely absorptive signal (a) at later times (Figure 4B).²² In Figure 4A the transient EPR spectrum of the triplet state of BChl *a* in an organic solvent²³ is included for comparison (dashed line). The early spectrum in the LH2 sample closely resembles the BChl *a* triplet spectrum.

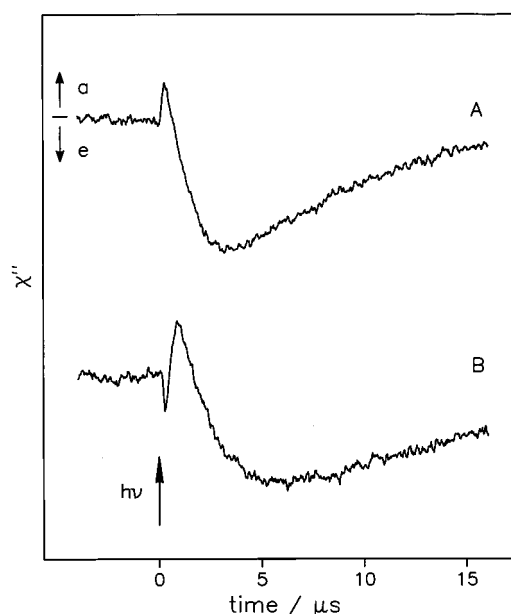


Figure 3. Time evolution of the EPR signals in LH2 complexes from *Chr. purpuratum* (A) and *Rb. sphaeroides* 2.4.1 (B). The transients were recorded at the *x* canonical field positions (335.2 mT and 332.1 mT for *Chr. purpuratum* and *Rb. sphaeroides* 2.4.1, respectively). The transient for *Chr. purpuratum* shows one polarization change from absorption (a) to emission (e). The transient for *Rb. sphaeroides* 2.4.1 shows at early times an additional polarization change from emission (e) to absorption (a). Experimental conditions: $T = 50$ K; microwave frequency $\nu = 9.71$ GHz; 30 dB microwave power attenuation; 1024 transients averaged for each trace.

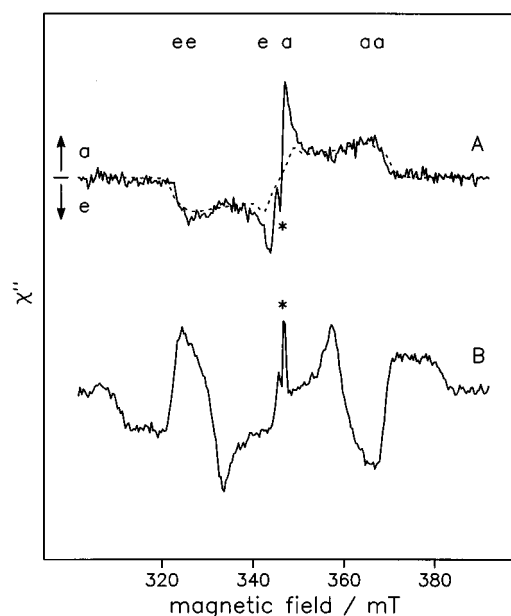


Figure 4. Transient EPR spectra of LH2 from *Rb. sphaeroides* 2.4.1 obtained at different times after light excitation. A (full line): spectrum in the time interval from 100 to 250 ns. B: spectrum in the time interval 2.0 to 3.5 μ s after the laser flash. A (dotted line): spectrum of the BChl *a* triplet state in an organic solvent. Experimental conditions: $T = 50$ K; microwave frequency $\nu = 9.71$ GHz; 30 dB microwave power attenuation; 256 magnetic field points; 1024 transients averaged per field point.

The D and E values given above are close to those for the BChl *a* triplet state in an organic solvent. This similarity leads us to an assignment of the early spectrum in the LH2 sample to a BChl *a* triplet state. This is consistent with the absorption flash photolysis data presented below.

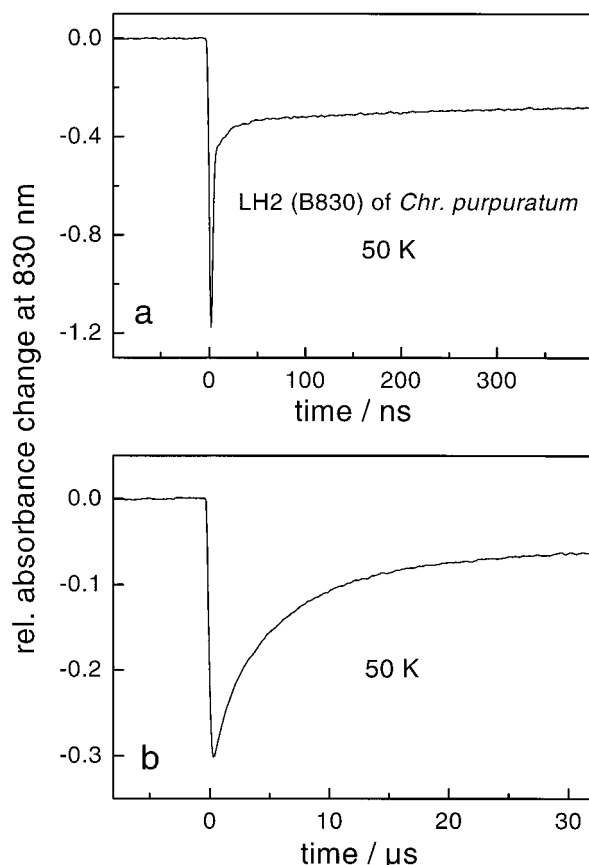


Figure 5. Time course of flash-induced absorbance changes at 830 nm of LH2 complexes from *Chr. purpuratum* monitored at and $T = 50$ K on a ns (a) and μ s (b) time scale.

In the cases of the LH2 samples from *Rb. sphaeroides* strains 2.4.1 and G1C, the carotenoid triplet formation detected by EPR was found to be strongly temperature dependent (data not shown). Due to the multiphasic kinetics, we did not attempt to analyze this temperature dependence on the basis of the EPR data alone but decided to use optical absorbance difference spectroscopy as well.

3.2. Time-Resolved Absorbance Difference Spectroscopy.

At first we describe the data from the LH2 (B830) complex from *Chr. purpuratum*. Figures 5a and 5b show the time course of the laser flash induced absorbance changes at 830 nm measured at $T = 50$ K. The very rapid transient (see Figure 5a) reflects the instrumental response to the following unresolved photoreactions. The initial bleaching is ascribed to the depletion of the ground state upon forming the first excited singlet state, which is partly converted into the triplet state by intersystem crossing. The BChl *a* triplet state then decays (too fast to be resolved) by triplet energy transfer to the carotenoid. This assignment is supported by the rapid, instrument-limited absorbance increase at 620 nm due to the formation of the carotenoid triplet (see Figure 6a). Most of the residual bleaching at 830 nm decays with the same time constant as the decay of the carotenoid triplet state (compare Figs. 5b and 6b). Previous work with this complex showed that there is an interaction between the carotenoids and the B830 BChl *a*'s such that the presence of the carotenoid triplet state induces a shift of the B830 Q_y absorption band.¹⁴ This shift then disappears as the carotenoid triplet state decays. A small part of the absorbance change at 830 nm decays in the ms time range (not shown) attributed to the decay of the secondary radical pair, $P^+Q_A^-$, in the reaction center portion of the sample. The decay of the initial

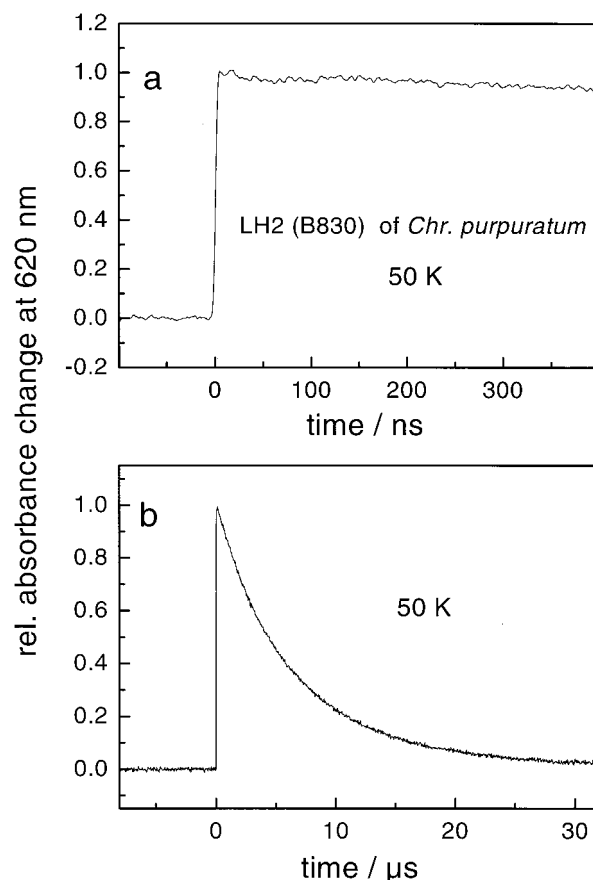


Figure 6. Time course of flash-induced absorbance changes at 620 nm of LH2 complexes from *Chr. purpuratum* $T = 50$ K on a ns (a) and μ s (b) time scale.

TABLE 2: Kinetics of the ^3Car Decay in the LH2 (B830) Complexes from *Chr. purpuratum*^a

T/K	$T1/\mu\text{s}$	$A1/\%$	$T2/\mu\text{s}$	$A2/\%$	$A3/\%$
5	3.4	76.4	18	23.6	
20	3.2	76.2	12	23.8	
50	3.4	73.5	9	26.5	
80	3.4	74	8.1	26	
130	4.2	99.4			0.6
180	4.1	99.5			0.5
240	3.5	98.7			1.3
270	3.0	98.7			1.3
293	1.2	96.8			3.2

^a The decay of the flash-induced absorbance changes at 620 nm were fitted with two exponentials plus an apparently nondecaying component. The half-lives ($T1$, $T2$) and relative amplitudes ($A1$, $A2$, $A3$) are given as a function of temperature. At all temperatures the time resolution of the apparatus was insufficient to resolve the rise kinetics of ^3Car . At all temperatures except at 293 K the sample contained 60% (v/v) glycerol.

bleaching at 830 nm (the $^3\text{BChl } a \rightarrow ^3\text{Car}$ reaction) and the rise of the carotenoid triplet signal (at 620 nm) were measured as a function of temperature from $T = 5$ K to room temperature (293 K). At all temperatures, the rate of carotenoid triplet formation was too fast to be resolved, i.e., faster than 3 ns, in agreement with a previous study.¹⁴ The decay of the triplet state showed a small temperature dependence (Table 2) but was kinetically complex at lower temperatures. Below $T = 100$ K, the decay was biphasic. At $T = 5$ K, for example, about 75% of the change decayed with a half-life of 3.4 μ s and the remaining 25% with a half-life of 18 μ s. Due to the slowing down of spin–lattice relaxation at low temperatures, the triplet sublevels are uncoupled and the different decay rates of the zero-

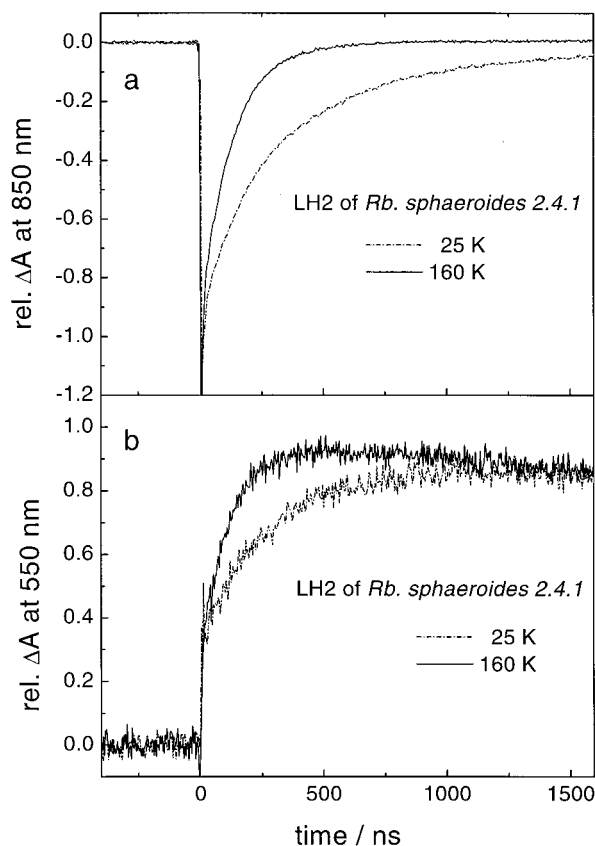


Figure 7. Time course of flash-induced absorbance changes of LH2 complexes from *Rb. sphaeroides* 2.4.1 monitored at (a) $\lambda = 850$ nm and (b) $\lambda = 550$ nm at $T = 25$ and 160 K.

field sublevels can be resolved. Above $T = 100$ K the decay was more monophasic with a half-life of 3–4 μ s. The faster decay at room temperature with $t_{1/2} \approx 1.2$ μ s is attributed to the accelerated intersystem crossing of carotenoids in the presence of oxygen.

In contrast to the situation with LH2 from *Chr. purpuratum*, the decay of the BChl *a* triplet and the rise of the carotenoid triplet in LH2 from *Rb. sphaeroides* 2.4.1 could be time resolved. Flash-induced absorbance changes at 850 nm attributed to the formation and decay of the BChl *a* triplet state were measured as a function of temperature from $T = 5$ to 293 K. Figure 7a shows the time course of the absorbance changes at $T = 25$ K and $T = 160$ K. The rise of the carotenoid triplet state has been followed at 550 nm (see Figure 7b). The decay of the BChl *a* triplet state is biphasic with half-lives of 143 and 414 ns at 25 K and 66 and 114 ns at 160 K. The amplitudes of both exponential phases are about equal.

The initial fast phase in the signals at 550 nm arises from the fact that excited states of BChl *a* also cause an absorbance increase at this wavelength.⁴ However, the differential molar extinction coefficient for the formation of the carotenoid triplet state is larger at this wavelength than that for the formation of the BChl *a* triplet state. Therefore, the rise of the carotenoid triplet state can be followed by the absorbance increase⁴ that is clearly resolved on the nanosecond time scale depicted in Figure 7b. At both temperatures, the rise of the carotenoid triplet state could also be fitted with two exponentials using virtually the same half-lives as obtained for the BChl *a* triplet decay (see above).

The triplet–triplet exchange reaction is strongly temperature dependent. At all temperatures there is an excellent kinetic match between the decay of the BChl *a* triplet state and the rise of the

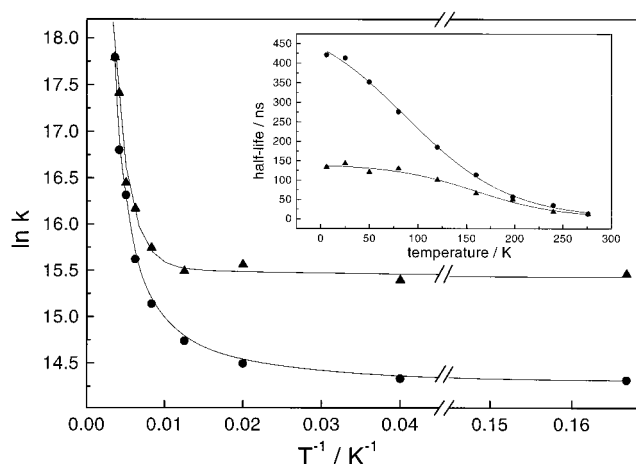


Figure 8. Temperature dependence of the time constants obtained from a two-exponential fit of the decay of $^3\text{BChl } a$ monitored at 850 nm for LH2 from *Rb. sphaeroides* 2.4.1. The logarithm of the decay constants $\ln k$ is plotted against the reciprocal temperature T^{-1} . The inset shows the half-lives $T_{1/2} = k^{-1}$ as a function of the temperature T .

carotenoid triplet state. This is the first direct demonstration of this kinetic correspondence in bacterial antenna complexes and confirms the direct triplet–triplet exchange reaction that has been postulated frequently in the past (for example, see refs 3, 4, 7). The temperature dependence of the kinetics of the BChl *a* triplet decay and of the carotenoid triplet rise is summarized in Figure 8. In Figure 8, the rate constants of the two phases obtained by biexponential fits of the $^3\text{BChl } a$ decay are depicted on a logarithmic scale as a function of the reciprocal temperature. The inset shows the half-lives of both phases as a function of the temperature. At low temperatures, the fit yields about equal amplitudes of both exponential phases. Above 160 K, an amplitude ratio of about 1 was kept fixed during the fit. The Arrhenius plot reveals a thermally activated triplet energy transfer in the range between 300 and 150 K corresponding to an activation energy of about 80 meV. At low temperatures ($T \leq 100$ K) the rate of the triplet energy transfer is rather temperature independent.

The decay of the carotenoid triplet state shows just as for *Chr. purpuratum* a weak temperature dependence. Above 50 K, the half-life is about 7 μ s. Again, at room temperature a faster decay with $t_{1/2} \approx 2.1$ μ s is observed. For *Rb. sphaeroides* 2.4.1, the carotenoid decay becomes clearly biphasic below $T = 20$ K. The half-lives at $T = 6$ K are 6.0 μ s and 28 μ s with relative amplitudes of about 75% and 25%, respectively.

Unlike the case with the LH2 complex of *Chr. purpuratum*, there is a weaker carotenoid/B850 interaction¹⁴ so that the bleaching at 850 nm decays very nearly to the baseline in the nanosecond time domain, i.e., parallel with the formation of the carotenoid triplet state.

The kinetics of the $^3\text{BChl } a \rightarrow ^3\text{Car}$ triplet energy transfer in the LH2 complexes from *Rb. sphaeroides* G1C is also well resolved on the nanosecond time scale (see Figure 9). But in this case, the temperature dependence is even more pronounced. The comparison between the kinetics of the BChl *a* triplet decay measured at 850 nm and of the carotenoid triplet rise measured at 515 nm shows again an excellent correspondence (see Figure 9). Multiexponential fits of the $^3\text{BChl } a$ decay at $T = 5$ K yielded the following half-lives and relative amplitudes: 220 ns (50%), 1600 ns (24%), 9.5 μ s (10%), and 42 μ s (16%). Half-lives of about 220 ns and 1600 ns are required to describe the formation of the carotenoid triplet state. Therefore, these phases

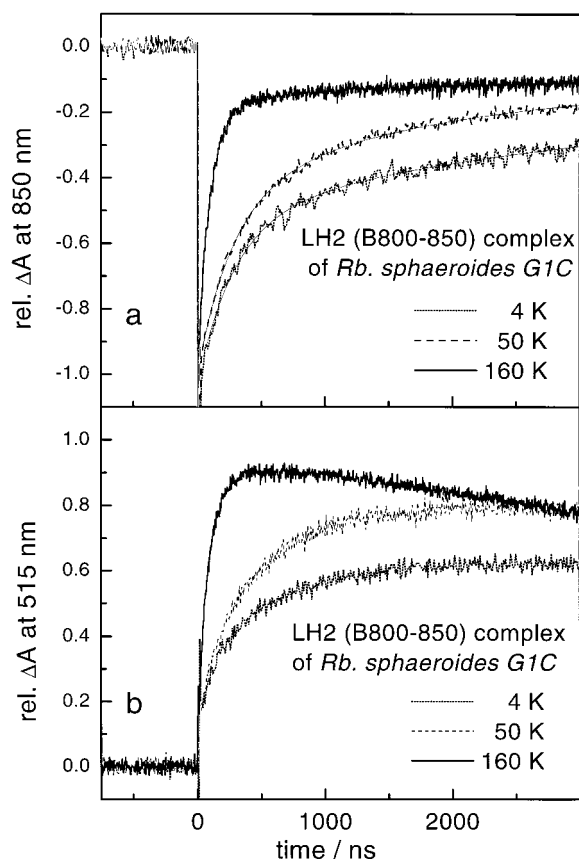


Figure 9. Time course of flash-induced absorbance changes of LH2 complexes from *Rb. sphaeroides* G1C monitored at (a) $\lambda = 850$ nm and (b) $\lambda = 515$ nm at $T = 4, 50$, and 160 K.

obviously reflect the $^3\text{BChl } a \rightarrow ^3\text{Car}$ triplet energy transfer. At all temperatures, a decay component of $^3\text{BChl } a$ with a half-life characteristic for the decay of the carotenoid triplet can be resolved. Therefore, the phase with $t_{1/2} \approx 9.5 \mu\text{s}$ at 5 K is assigned to the carotenoid/BChl a interaction in the LH2 complex of *Rb. sphaeroides* G1C. The half-life of about $42 \mu\text{s}$ is similar to that observed for the decay of $^3\text{BChl } a$ in solution (see, e.g., ref 24). In *Rb. sphaeroides* R-26, which lacks carotenoids, the BChl a triplet state of LH2 decays with $t_{1/2} \approx 70 \mu\text{s}$ at room temperature.⁴ Most probably the $t_{1/2} \approx 42 \mu\text{s}$ phase reflects both, a slow triplet energy transfer from BChl a to carotenoid and the intrinsic decay of the BChl a triplet state by intersystem crossing. Therefore, the slowest phase indicates that the BChl a triplet state is not completely quenched by triplet energy transfer. As a consequence, the yield of carotenoid triplet formation is reduced. This is consistent with the observations in the time-resolved EPR experiments where signal contributions from the BChl a triplet state are visible beyond $10 \mu\text{s}$ after the laser flash (see Figure 1D). A similar freezing out of carotenoid triplet formation has been previously reported for reaction centers of *Rb. sphaeroides* containing neurosporene²⁵ and for LHCII of higher plants.²⁶

Figure 10 shows the decay kinetics of the carotenoid triplet state measured on a μs time scale. At 4 K, the decay is again clearly biphasic with half-lives of $9.5 \mu\text{s}$ (61%) and $43 \mu\text{s}$ (39%). Above 50 K, the decay can be described by one exponential with a half-life that decreases slightly from $9.8 \mu\text{s}$ at 50 K to $8 \mu\text{s}$ at 190 K. At room temperature in the presence of oxygen we observe $t_{1/2} \approx 3.3 \mu\text{s}$. The inset of Figure 10 shows the temperature dependence of the extrapolated initial amplitude. The reduced amplitude probably reflects a reduced carotenoid triplet yield at low temperature, as discussed above. A quantita-

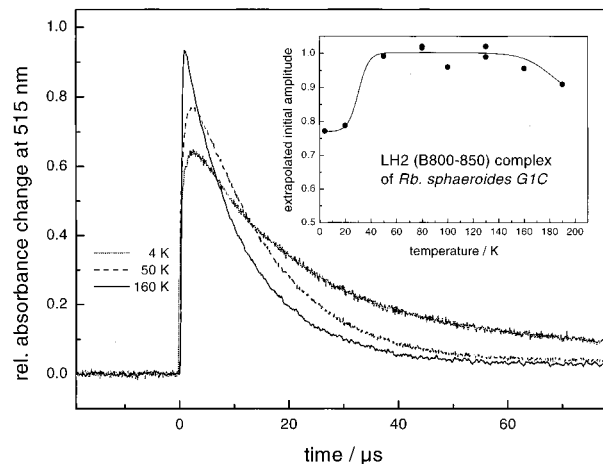


Figure 10. Time course of flash-induced absorbance changes of LH2 complexes from *Rb. sphaeroides* G1C monitored at $\lambda = 515$ nm on a μs time scale and at $T = 4, 50$, and 160 K. The inset shows the temperature dependence of the extrapolated initial amplitude of the component decaying on the μs time scale.

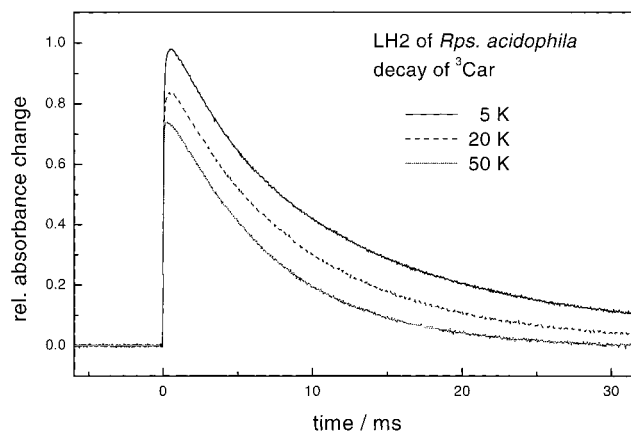


Figure 11. Decay of the carotenoid triplet state in LH2 complexes from *Rps. acidophila* monitored by the absorbance change at 550 nm and $T = 5, 20$, and 50 K. The amplitude for the trace at $T = 5$ K has been normalized to 1. The amplitudes of the relative absorbance changes decrease with increasing temperature.

tive analysis is, however, complicated by the fact that the differential molar extinction coefficient for the carotenoid triplet formation will increase with decreasing temperature as the absorption bands become narrower at lower temperatures.^{3,4} This effect is seen in Figure 11 (see below) for the LH2 complex from *Rps. acidophila*, where as the temperature is lowered the flash-induced absorbance change due to the carotenoid triplet formation increases though the yield is largely temperature independent.

With the LH2 complexes from *Rps. acidophila*, the $^3\text{BChl } a \rightarrow ^3\text{Car}$ triplet energy transfer could be well resolved for temperatures below 50 K. Again, the decay kinetics of the BChl a triplet state was measured by absorbance changes at 850 nm, whereas the formation and decay of the carotenoid triplet state was followed by absorbance changes at 550 nm. Table 3 gives the time constants and relative amplitudes describing the kinetics of the $^3\text{BChl } a \rightarrow ^3\text{Car}$ energy transfer at $T = 5, 20$, and 50 K. At all temperatures, the absorbance change at 850 nm decays entirely in the nanosecond time domain indicating (i) that the carotenoid/BChl a interaction is weak in LH2 complexes of *Rps. acidophila*¹⁴ and (ii) that the BChl a triplet state is virtually completely quenched by the triplet energy transfer to the carotenoid at all temperatures investigated. Nevertheless, the

TABLE 3: Decay Kinetics of ³BChl *a* in LH2 Complexes from *Rps. acidophila* 10050^a

<i>T</i> /K	<i>T</i> ₁ /ns	<i>A</i> ₁ /%	<i>T</i> ₂ /ns	<i>A</i> ₂ /%
5	26	47	126	51
20	21	50	104	49
50	10	82	59	18
> 80	< 10	> 95		

^a Analyzed by two-exponential fits (plus a constant) yielding half-lives *T*₁, *T*₂ and amplitudes *A*₁ and *A*₂, respectively.

amplitude of the absorbance change due to carotenoid triplet formation depends strongly on the temperature. Figure 11 shows the decay of the carotenoid triplet state with a nearly temperature independent half-life of about 5 μs. The increase of the extrapolated initial amplitude with decreasing temperature is attributed to the fact that the differential molar extinction coefficient for carotenoid triplet formation will increase with decreasing temperature as the absorption bands become narrower at lower temperatures,^{3,4} as discussed above.

4. Discussion

Time-Resolved EPR. The transient EPR data presented above show a common polarization inversion phenomenon during the lifetime of the spin-polarized carotenoid triplet states in LH1 and LH2 preparations from different purple bacteria. There are two obvious possible reasons for this observation. On one hand, there could be a carotenoid–carotenoid triplet exchange reaction occurring during the lifetime of the carotenoid triplet state. If, for example, the antenna sample contained two different populations of carotenoids then, in principle, this type of triplet–triplet exchange reaction could lead to a change in spin polarization. It would have to be assumed in this case, that the relative positions of the carotenoid triplet state axes in space are different. Now the projection of the precursor triplet onto the molecular frame of the acceptor triplet would result in a changed population difference of its three triplet state sublevels relative to the precursor triplet state. In the case of the LH1 complex from *R. rubrum* studied here and the LH2 complex from *Rps. acidophila* studied here and in ref 15, this can be definitely ruled out because each αβ apoprotein pair in these complexes only binds a single carotenoid molecule.²⁷ There is not another carotenoid close enough to allow a triplet–triplet energy transfer to occur within the carotenoid triplet state lifetime of a few μs. The other alternative suggested in ref 15 is that the projection of the precursor BChl *a* triplet state onto the molecular frame of the carotenoid initially sets up a given pattern of spin polarization. Then, due to different decay rates of the three triplet sublevels of the carotenoid to the ground state, the spin polarization pattern evolves during the total triplet state lifetime.

The transient absorbance data show that the decay of the carotenoid triplet states is rather temperature independent, for example between 293 and 6 K the decay of the carotenoid triplet state in LH2 from *Rb. sphaeroides* 2.4.1 only slows down from ≈ 2 to ≈ 9.4 μs. In the absorption experiment, the total triplet population is monitored and is less sensitive to differences in the sublevel decay time constants. Only one overall decay time constant is observed at temperatures above 100 K. Only at temperatures below 100 K is spin–lattice relaxation slow enough to give rise to a multiphasic decay of the triplet population. The model using different triplet sublevel decay rates¹⁵ to account for the polarization inversion seen in the time-resolved EPR experiment requires that one of the sublevels decays at least as fast as the polarization inverts, i.e., with a

half-life of about 1.2 μs. In the transient absorption, no such fast decay phase has been observed. At present we cannot give an explanation for this apparent inconsistency.

The transient EPR signals show in the case of LH2 from *Rb. sphaeroides* a kinetic phase which we assign to the triplet energy transfer from BChl *a* to the carotenoid. This assignment is based on the similarity of the very early transient spectra in LH2 to the spectrum of BChl *a* in an organic solvent. The zero-field splitting parameters *D* and *E* for the BChl *a* triplet state in LH2 closely resemble those of the BChl *a* triplet state in an organic solvent. This is in contrast to the situation for the primary donor triplet state ³P₈₆₅ in reaction centers of *Rb. sphaeroides* with reduced *D* and *E*. The reduction of *D* and *E* reflects the delocalization of the triplet state over both BChl *a* molecules of the dimeric primary donor P₈₆₅. For the “special pair” P₈₆₅ in particular *E* is reduced due to the in-plane rotation of the two BChl *a* molecules with respect to each other. A similar rotation of the BChl *a* planes in the B850 ring between α- and β-bound BChl *a* is observed in the X-ray structure of LH2 from *Rps. acidophila*.¹¹ Because no reduction of *E* is observed for the BChl *a* triplet in LH2 of *Rb. sphaeroides* at low temperatures, we conclude that the triplet state is localized on one individual BChl *a* molecule in the B850 ring and no hopping of the triplet state between neighboring BChl *a* occurs on a time scale much faster than the overall BChl *a* to carotenoid triplet energy transfer. Even though the arrangement of the BChl *a* in the special pair and the B850 ring are grossly similar, there are enough differences in detail that could explain the changed properties of the triplet states. The localization of the triplet state on one BChl *a* in the B850 ring has implications for the interpretation of the complex temperature dependence of the BChl *a* to carotenoid triplet energy transfer observed in the transient absorption experiments, which will be discussed now.

Time-Resolved Absorbance Difference Spectroscopy. Both time-resolved EPR and optical absorption spectroscopy data presented above clearly show that the carotenoid triplet state in all of the antenna complexes studied is formed by a direct triplet–triplet exchange reaction with the BChl *a* triplet state. The kinetic correspondence required by this mechanism is observed at all temperatures studied for those species with a ns rise time of the carotenoid triplet state. Moreover, the donor BChl *a* triplet state resides on the BChl *a* molecules that constitute the large, tightly coupled ring of chromophores seen in the structures of both LH2 and LH1,^{11,28,29} since the bleaching due to the BChl *a* triplet state in the near infrared is in the long wavelength absorption band of the antenna complexes.

Chromatium purpuratum. In the case of *Chr. purpuratum*, the triplet energy transfer from the BChl *a* to the carotenoid was too fast to be resolved on a nanosecond time scale at all temperatures down to liquid helium temperature. This extremely fast triplet energy transfer is consistent with the observed strong interaction between BChl *a* and carotenoid in this LH2 complex visible as a shift of the B830 BChl *a* Q_y absorption band in the presence of the carotenoid triplet state.¹⁴

Rhodobacter sphaeroides. In the cases of the LH2 complexes from *Rb. sphaeroides* strains G1C and 2.4.1 and *Rps. acidophila* strain 10050 (for *T* < 80 K) the kinetics of the decay of the BChl *a* triplet state and the rise-time of the carotenoid triplet state could be easily resolved.

The kinetics of the triplet energy transfer and its temperature dependence are complex in all cases. If we concentrate first on the rise-kinetics of carotenoid triplet formation in the LH2 complex from *Rb. sphaeroides* strain 2.4.1, then initially at *T* = 160 K and above the rise-kinetics are satisfactorily fitted by

a single exponential. Below $T = 160$ K, the residuals indicate significant deviations of the triplet energy transfer from a first-order process, and two exponentials were required for a satisfactory fit. Similar behavior is seen for the corresponding decay of the BChl *a* triplet state. As the temperature is lowered from room temperature to about 150 K, the rate of carotenoid triplet formation decreases, in agreement with previous work.¹⁴ Below 100 K, the rate of triplet energy transfer is nearly temperature independent. How can this behavior be explained? The Dexter formulation of the electron exchange mechanism for a standard triplet–triplet exchange reaction, especially in a quasi-solid-state case like this, does not have a very explicit temperature-dependent term.⁸ The Dexter equation does have an “effective” spectral overlap (or energy gap) term, and if this is temperature dependent then it could contribute to the temperature dependence seen, e.g., in Figure 8.

The absorption spectra of LH2 complexes are temperature dependent (for example, see ref 30). As the temperature is lowered the 850 nm absorption band narrows and shifts to the red as do the carotenoid absorption bands in the visible region of the spectrum. However, these spectral changes are not a continuous function of temperature. The spectral shift is essentially complete by 150 K, whereas the narrowing of the band is even more pronounced at temperatures below 150 K. As seen in Figure 8, the most prominent temperature dependence of the transfer rate occurs in the temperature range from room temperature to $T \approx 150$ K ($T^{-1} \leq 0.007$). At lower temperatures, two rate constants with similar amplitudes are resolved. The faster rate constant shows a minor temperature dependence below $T \approx 100$ K. In contrast, the slower rate shows a clear temperature dependence down to about 50 K.

The biphasic kinetics of the triplet energy transfer from BChl *a* to the carotenoid can be understood on the basis of the structure of the LH2 complex. The X-ray structure of LH2 from *Rps. acidophila* strain 10050 shows a single carotenoid present per $\alpha\beta$ -apoprotein pair, and the π -system of this carotenoid only comes into van der Waals contact with the π -system of one of the two B850–BChl *a* molecules present in that $\alpha\beta$ -apoprotein dimer^{11,31} (Figure 12). On the basis of the analogous distance difference between the carotenoid and the α - and β -bound B850–BChl *a*s in *Rhodospirillum rubrum*²⁸ an effective triplet quenching of the former and an ineffective direct quenching for the latter have been predicted from quantum chemical calculations of energy transfer in LH2.³² An effective indirect quenching of triplet states on β -bound BChl *a* must proceed via a fast triplet transfer from the β -bound to the α -bound BChl *a* and subsequent transfer to the carotenoid. The calculated triplet transfer time constant from the β -bound to the α -bound BChl *a* is faster than the calculated transfer from the α -bound BChl *a* to the carotenoid.³² Irrespective of the fact that the transfer time from the α -bound BChl *a* to the carotenoid calculated for *R. rubrum* is about 2 orders of magnitude slower than observed here for species with resolvable triplet transfer kinetics on the nanosecond time scale, we assume that at temperatures above about 150 K the triplet energy transfer between β - and α -bound B850 BChl *a* is fast and the rate-limiting step is the triplet energy transfer from the α -bound BChl *a* to the carotenoid. At temperatures below about 150 K, the triplet transfer from the β -bound BChl *a* to the α -bound BChl *a* apparently becomes slower than the transfer from the α -bound BChl *a* to the carotenoid giving rise to the slower observed kinetic phase. A slow triplet transfer from β -bound to α -bound B850 BChl *a* is consistent with the observation of



Figure 12. Arrangement of the B850 BChl *a* and the carotenoid in the LH2 complex from *Rps. acidophila*.³¹ The carotenoid passes over the face of the α -bound BChl *a* of the B850 ring.

a BChl *a* triplet state localized on an individual BChl *a* molecule in the time-resolved EPR experiments at low temperatures.

The temperature dependence between room temperature and about 150 K can be rationalized by assuming a change of the “effective” spectral overlap of the BChl *a* phosphorescence spectrum and the direct carotenoid phosphorescence excitation spectrum concomitant with the red shift of the absorption spectrum from room temperature to 150 K. However, the slowing down of the triplet transfer from the β -bound to the α -bound BChl *a* at temperatures lower than about 150 K cannot be attributed to spectral shifts. One possible explanation would be a difference in the triplet energies of the α - and the β -bound BChl *a*. Different singlet transition energies of both BChl *a* species have been invoked in some of the most recent calculations of the spectroscopic properties of LH2 based on the structure (see, e.g., ref 33). These calculations suggest that an individual α -bound B850 BChl *a* molecule would absorb at about 803 nm and an individual β -bound B850 BChl *a* molecule at 823 nm. If a difference between the triplet energies of α -bound and β -bound B850 BChl *a* exists with a lower triplet energy of the β -bound B850 BChl *a*, then the triplet energy transfer from the β -bound BChl *a* to the carotenoid via the α -bound BChl *a* would involve an energy uphill step. This model implies a freezing out of the triplet energy transfer at low temperatures. This contradicts the observed small temperature dependence of the slow rate at temperature below 50 K. A freezing out of an uphill triplet energy transfer is observed for the triplet transfer in bacterial reaction centers from the primary donor P_{865} to a carotenoid via a monomeric BChl *a*. There the triplet energy transfer is effectively blocked at temperatures below 38 K,²⁵ consistent with the estimated activation energy of about 200 cm^{-1} ³⁴ for the step from $^3P_{865}$ to the monomeric BChl *a*. If, however, the triplet energy of the α -bound B850 BChl *a* is lower than that of the β -bound molecule, the observed temperature dependence of the slow triplet energy transfer rate can be explained. The narrowing of

the of the B850 absorption band continues down to temperatures below 50 K and seems to stop only below about 20 K.³⁰ This might be associated with a decreasing overlap of the phosphorescence spectrum of the β -bound B850 BChl *a* and the phosphorescence excitation spectrum of the α -bound BChl *a*, which governs the triplet energy transfer between both molecules. An alternative explanation might be a decrease in the electronic coupling between neighboring B850 BChl *a* molecules. However, analysis of the thermal broadening of the B850 absorption indicated an increase of the monomer–monomer couplings with decreasing temperature.³⁰

Because the qualitative temperature dependence of the triplet energy transfer in LH2 from *Rb. sphaeroides* strain G1C is similar to the case of *Rb. sphaeroides* strain 2.4.1, the arguments given also hold. Quantitatively, the temperature dependence in G1C is stronger than in 2.4.1. In LH2 from *Rb. sphaeroides* strain 2.4.1, the fast phase for the carotenoid triplet rise at 5 K is about 10 times slower than the rise at room temperature. In LH2 from *Rb. sphaeroides* strain G1C, the fast phase at 5 K is about 20 times slower than the room-temperature kinetics. Even more pronounced is the difference in the slow low-temperature phase. Whereas in 2.4.1 the slow phase at 5 K is about 30 times slower than the room-temperature triplet rise, in G1C the slow phase is about 3 orders of magnitude slower. In addition, we observe in LH2 from G1C a partial freezing out of the triplet energy transfer from BChl *a* to the carotenoid occurs at low temperatures.

Obvious candidates for an explanation of these differences might be the different carotenoids in these two strains. While LH2 from *Rb. sphaeroides* strain 2.4.1 contains the carotenoid spheroidene with 10 conjugated double bonds in the polyene chain, *Rb. sphaeroides* strain G1C contains neurosporene with 9 conjugated double bonds. The shorter carotenoid has a higher triplet energy than the longer one. This might result in a partial energetic inaccessibility of the carotenoid triplet state of the shorter carotenoid. However, even for neurosporene with 9 conjugated double bonds, the triplet energy is much lower than for BChl *a*. Therefore, the difference between *Rb. sphaeroides* strains 2.4.1 and G1C cannot easily be explained on the basis of the energetics of the respective carotenoids. Secondary effects induced by the altered carotenoid in *Rb. sphaeroides* G1C might change the triplet energies of β - and α -bound B850 BChl *a* compared to *Rb. sphaeroides* 2.4.1. If the difference of the triplet energies of β - and α -bound B850 BChl *a* is in the case of *Rb. sphaeroides* G1C smaller than the energetic heterogeneity of the individual BChl *a* triplet energies, then part of the β -bound BChl *a* will have a smaller triplet energy than the neighboring α -bound BChl *a*. An energetic heterogeneity of the singlet transition energies of B850 BChl *a* has been invoked to explain the excitonic structure of the B850 ring (see, e.g., ref 35). For those β -bound BChl *a* with triplet energy smaller than the neighboring α -bound BChl *a* the triplet energy, transfer to the carotenoid via the α -bound BChl *a* is blocked at low temperature.

Rhodospseudomonas acidophila. Finally we turn to the situation found in the LH2 complex from *Rps. acidophila*. The BChl *a* \rightarrow carotenoid triplet energy transfer could be resolved in this complex only at temperatures below 50 K. At 5 K the rise of the carotenoid triplet state is biphasic, as seen in the LH2 complexes from *Rb. sphaeroides*. However, both phases are much faster in *Rps. acidophila*, with the slow time constant in *Rps. acidophila* being similar to the fast one in *Rb. sphaeroides* strain 2.4.1. The differences in the rate constants are in agreement with differences observed for LH2 from *Rps.*

acidophila and *Rb. sphaeroides* in absorption and hole burning experiments.³⁰ An overall similarity of the properties of both LH2 complexes has been found. However, a difference in the nearest neighbor BChl *a*–BChl *a* couplings was deduced, with the coupling in *Rb. sphaeroides* being about 20% weaker than in *Rps. acidophila*. This reduced coupling was associated with a looser packing of the α,β -polypeptide pair in *Rb. sphaeroides*. Such a difference in packing would not only explain a faster triplet energy transfer in *Rps. acidophila* between the β - and α -bound B850 BChl *a* but also a better coupling between the α -bound B850 BChl *a* and the carotenoid leading to a faster BChl *a* to carotenoid triplet energy transfer.

5. Conclusions

We have demonstrated the direct triplet energy transfer from BChl *a* in the tightly coupled ring in antenna complexes from purple bacteria to the carotenoids. The time-resolved EPR spectra of the ³BChl *a*, precursor state of the carotenoid triplet, are indicative of a triplet state localized on one individual BChl *a* within the ring. The rate constant for the triplet energy transfer is strongly temperature and species dependent. At low temperatures biphasic kinetics for the rise of the carotenoid triplet state has been found. A likely origin for this biphasic kinetics is the arrangement of BChl *a* and carotenoids in the LH2 complexes. Only the α -bound BChl *a* molecule present in an $\alpha\beta$ -apoprotein dimer comes with its π -system in van der Waals contact with the π -system of a carotenoid, allowing efficient triplet energy transfer. The β -bound BChl *a* molecule shows a larger distance to a carotenoid and, therefore, a drastically reduced direct triplet energy transfer efficiency is expected. An essential assumption for the explanation of the observed temperature dependence in terms of the structure of the LH2 complexes is a slightly higher triplet energy of the α -bound BChl *a* molecules compared to that of the β -bound BChl *a* molecules. The slower triplet energy transfer in LH2 complexes from *Rb. sphaeroides* than in complexes from *Rps. acidophila* has been attributed to a different packing of the α,β -polypeptide pairs. A better understanding of the observed temperature and species dependence of BChl *a* to carotenoid triplet energy transfer requires further comparative theoretical and experimental studies on the two species *R. sphaeroides* and *R. molischianum* with known structure.

Acknowledgment. We are grateful to Professors H. A. Frank (University of Connecticut) and R. van Grondelle (Vrije Universiteit Amsterdam) for stimulating discussions. This work was supported by the Alexander von Humboldt-Stiftung (fellowship to R.J.C.), Deutsche Forschungsgemeinschaft (Sfb 498, TP A1, C5), and Fonds der Chemischen Industrie (to R.B. and W.L.).

References and Notes

- (1) Frank, H. A.; Cogdell, R. J. *Photochem. Photobiol.* **1996**, *63*, 257.
- (2) Koyama, Y.; Kuki, M.; Andersson, P. O.; Gilbro, T. *Photochem. Photobiol.* **1996**, *63*, 243.
- (3) Cogdell, R. J.; Monger, T. G.; Parson, W. W. *Biochim. Biophys. Acta* **1975**, *408*, 189.
- (4) Monger, T. G.; Cogdell, R. J.; Parson, W. W. *Biochim. Biophys. Acta* **1976**, *449*, 136.
- (5) Cogdell, R. J.; Hipkins, M. F.; MacDonald, W.; Truscott, T. G. *Biochim. Biophys. Acta* **1981**, *634*, 191.
- (6) Foote, C. S.; Chang, Y. C.; Denny, R. W. *J. Am. Chem. Soc.* **1970**, *92*, 5216.
- (7) Cogdell, R. J.; Frank, H. A. *Biochim. Biophys. Acta* **1987**, *895*, 63.
- (8) Dexter, D. L.; *J. Chem. Phys.* **1953**, *21*, 836.

- (9) Yeates, T. O.; Komiya, H.; Chirino, A.; Rees, D. C.; Allen, J. P.; Feher, G. *Proc. Natl. Acad. Sci. U.S.A.* **1988**, *85*, 7993.
- (10) Deisenhofer, J.; Epp, O.; Sinning, I.; Michel, H. *J. Mol. Biol.* **1995**, *246*, 429.
- (11) McDermott, G.; Prince, S. M.; Freer, A. A.; Hawthornthwaite-Lawless, A. M.; Papiz, M. Z.; Cogdell, R. J.; Isaacs, N. W. *Nature* **1995**, *374*, 517.
- (12) Frank, H. A.; Bolt, J. D.; S. M. d. Costa, B.; Sauer, K. *J. Am. Chem. Soc.* **1980**, *102*, 4893.
- (13) Chadwick, B. W.; Frank, H. A. *Biochim. Biophys. Acta* **1986**, *851*, 257.
- (14) Angerhofer, A.; Bornhäuser, F.; Gall, A.; Cogdell, R. *J. Chem. Phys.* **1995**, *194*, 259.
- (15) Carbonera, D.; DiValentin, M.; Agostini, G.; Giacometti, G.; Liddell, P.; Gust, D.; Moore, A. L.; Moore, T. A. *Appl. Magn. Reson.* **1997**, *13*, 487.
- (16) McGann, W. J.; Frank, H. A. *Chem. Phys. Lett.* **1985**, *121*, 253.
- (17) Cogdell, R. J.; Hawthornthwaite, A. M. In *The Photosynthetic Reaction Center*; Deisenhofer, J., Norris, J. R., Eds.; Academic Press: San Diego, 1993; p 23.
- (18) Frank, H. A.; Chadwick, B. W.; Oh, J. J.; Gust, D.; Moore, T. A.; Liddell, P. A.; Moore, A. L.; Makings, L. R.; Cogdell, R. J. *Biochim. Biophys. Acta* **1987**, *892*, 253.
- (19) Hawthornthwaite, A. M.; Cogdell, R. J. In *Chlorophylls*; Scheer, H., Ed.; CRC Press: Boca Raton, 1991; p 493.
- (20) Proskuryakov, I. I.; Shkuropatov, I. B. K. A. Y.; Shkuropatova, V. A.; Shuvalov, V. A. *Biochim. Biophys. Acta* **1993**, *1142*, 207.
- (21) Snyder, S. W.; Morris, A. L.; Bondeson, S. R.; Norris, J. R.; Thurnauer, M. C. *J. Am. Chem. Soc.* **1993**, *115*, 3774.
- (22) Zech, S. G.; Gardiner, A. T.; Lubitz, W.; Bittl, R. In *Magnetic Resonance and Related Phenomena*; Ziessow, D., Lubitz, W., Lendzian, F., Eds.; Technische Universität Berlin: Berlin, 1998; Vol. II, p 949.
- (23) Lendzian, F.; Bittl, R.; Lubitz, W. *Photosynth. Res.* **1998**, *55*, 189.
- (24) Connolly, J. S.; Gorman, D. S.; Seely, G. R. *Ann. N. Y. Acad. Sci.* **1973**, *206*, 649.
- (25) Schenck, C. C.; Mathis, P.; Lutz, M. *Photochem. Photobiol.* **1984**, *39*, 407.
- (26) Peterman, E. J. G.; Dukker, F. M.; van Grondelle, R.; van Amerongen, H. *Biophys. J.* **1995**, *69*, 2670.
- (27) Arellano, J. B.; Bangar Raju, B.; Naqui, K. R.; Gillbro, T. *Photochem. Photobiol.* **1998**, *68*, 84.
- (28) Koepke, J.; Hu, X.; Münke, C.; Schulten, K.; Michel, H. *Structure*; **1996**, *4*, 581.
- (29) Karrasch, S.; Bullough, P. A.; Ghosh, R. *EMBO J.* **1995**, *14*, 631.
- (30) Wu, H.-M.; Ratsep, M.; Jankowiak, R.; Cogdell, R. J.; Small, G. *J. J. Phys. Chem. B* **1997**, *101*, 7641.
- (31) Prince, S. M.; Papiz, M. Z.; Freer, A. A.; McDermott, G.; Hawthornthwaite-Lawless, A. M.; Cogdell, R. J.; Isaacs, N. W. *J. Mol. Biol.* **1997**, *268*, 412.
- (32) Damjanović, A.; Ritz, T.; Schulten, K. *Phys. Rev. E* **1999**, *59*, 3293.
- (33) Koolhaas, M. H. C.; van der Zwan, G.; Frese, R. N.; van Grondelle, R. *J. Phys. Chem. B* **1997**, *101*, 7262.
- (34) Takiff, L.; Boxer, S. G. *J. Am. Chem. Soc.* **1988**, *110*, 4425.
- (35) Wu, H.-M.; Ratsep, M.; Lee, I.-S.; Cogdell, R. J.; Small, G. J. *J. Phys. Chem. B* **1997**, *101*, 7654.